Phase Relationships and Cation Disorder in $RE_{1+x}Ba_{2-x}Cu_3O_{7+\delta}$, RE = Pr, Nd, Sm, Gd

M. J. Kramer,* H. Wu,*# K. W. Dennis,* B.I. Polzin,* D.K. Falzgraf* and R. W. McCallum*#

*Ames Laboratory
#Department of Materials Science and Engineering
Iowa State University
Ames, IA 50011 U.S.A.

ABSTRACT

Unlike Y123 which forms only a stoichiometric compound, the light rare earth elements (LRE) form a solid solution $LRE_{1+x}Ba_{2-x}Cu_3O_{7+\delta}$ (LRE123ss), with increasing substitution of the LRE^{3+} for the Ba^{2+} as the ionic radii of the LRE increases. The sub-solidus phase relationships around the LRE123ss change for La, Pr and Nd, but are similar for Sm and Gd. However, the solubility limit decreases with decreasing ionic radii. In addition, the solubility limits for Sm and Gd are strongly influenced by PO_2 during high temperature annealing. The range of solubility is, for any given LRE system, strongly dependent on the oxygen partial pressure(PO_2) providing a new means by which to control the microstructure in the RE123 system.

Key Words: Light rare earth elements, solid-solution, oxygen partial pressure

INTRODUCTION

There has been increasing interest in the isostructural variants of $YBa_2Cu_3O_{7-d}$, in particular where the lighter rare-earth elements (RE) substitute for Y. The ionic radii of the light rare-earth elements (LRE) approaches that of the Ba [1], allowing for a large degree of substitution of the LRE^{3+} for Ba^{2+} without forming second phases. The formula can be written as $LRE_{1+x}Ba_{2-x}Cu_3O_{7+d}$ (LRE123ss). Considerable work has shown that the equilibrium phase diagram changes with LRE, in that LRE123 is no longer a point compound but shows varying amounts of solid solution [2-8]. In an earlier paper, it was demonstrated that the substitution of a LRE^{3+} for Ba^{2+} must be compensated for by the addition of extra O to maintain charge balance [9], thus the limits of solid solubility is a function of both ionic radii and oxygen partial pressure (PO_2) [10]. For the La123ss, there does not appear to be a dependency of the solubility limit over a span of 4 orders of magnitude in PO_2 ($0.02 < x < 0.7$) [3]. The Pr123ss and Nd123ss show a strong influence of PO_2 on the lower limit of solubility [7]. For Pr123ss the lower limit of x is ~ 0.01 at 0.001 bar PO_2 but this increases to nearly 0.04 for 1 bar PO_2. Nd123ss also showed that the lower limit of solubility was decreased with lower PO_2 (x from 0.04 to 0.0) but the upper limit was not changed (x = 0.6) over 3 orders of magnitude change in PO_2. The orthorhombic to tetragonal transition for fully oxygenated samples occurred at ~ x = 0.2 for the La123ss and at x = 0.25 for the Nd123ss for fully oxygenated samples. In both the La123ss and the Nd123ss, the peritectic decomposition temperatures are similar and both decrease with decreasing PO_2. In this paper we will review our previous work on the phase relations as a function of PO_2 in the Pr123ss and Nd123ss and include new results on the Sm123ss and Gd123ss systems.

EXPERIMENTAL PROCEDURES

Material Preparation

The materials for the present study were prepared by solid state reactions of RE_2O_3, $BaCO_3$, and CuO. The precursor powders were dried, weighed, and ground together in a micromill to sub-micron size. The materials were pressed into pellets, calcined twice in flowing CO_2 free air (flow rate ~ 10 *l*/min) for 24 hours at 890 to 900°C with an intermediate grinding and pressing. The materials were then sintered at temperatures ranging from 940 to 1025°C for > 24 hours in flowing oxygen (flow rate ~ 50 *ml*/min) then cooled to 450°C and held another 24 hrs. Smaller samples were then cut from these pellets and re-annealed at temperatures up to 950°C in 1% O_2 (99% N_2) for 24 hours then cooled to 450° and then soaked 24 hours in 100% flowing O_2. Details on the preparation of samples having sharp transitions and consistent Meissner's fractions were published elsewhere [8]. The annealing temperatures were varied in order to maintain a fairly constant homologous temperature (T/T_m) where T_m is the melting temperature. T_m is both a function of x and PO_2 and thus variable from system to system. The large cations have low diffusivity, therefore high temperatures are necessary to achieve homogeneity.

Material Characterization

All magnetization measurements were made using a DC SQUID magnetometer at 10 Oe. Monolithic samples of the same dimensions (6 x 1 x 1 mm) were cut from the center portion of the sintered pellets and measured with the long dimension parallel to the field to minimize demagnetization effects. XRD was performed on flat surface of the cut slabs or on powdered samples sieved to < 50 μm. Lattice parameters were determined using a least squares fitting program. Differential thermal analysis (DTA) was performed on ground powders at a heating rate of 10°C/min where the atmospheres were adjusted by electronic mass flow controllers to within 1% of the stated value. Since it is difficult to detect small amounts of second phases in XRD, the limits of solubility were determined in three ways: 1) changes in the lattice parameter as a function of x, 2) changes in the onset of the peritectic decomposition and 3) changes in the onset of the superconducting transition. The first two techniques should be sensitive to the structural limits of the solubility, the last should be only sensitive to the limit of solubility when superconductivity is present. However, there are intercalated structures (i.e., $YBa_2Cu_4O_8$ and $Y_2Ba_4Cu_7O_{15}$) which are difficult to detect with XRD but can be determined by DC SQUID magnetometry.

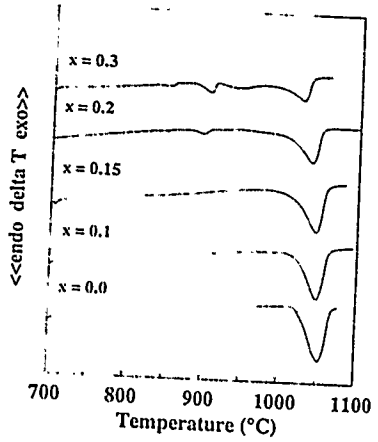

Fig. 1 DTA of Sm123ss performed in 1% O_2 balance N_2 showing the presence of a second phase occurring at x = 0.2.

RESULTS

Sm123

Previous work has shown that the solubility limit in the Sm123ss system processed in oxygen is $x \approx 0.7$, similar to that of La123ss, Pr123ss and Nd123ss [11,12]. This is surprising since there is a 21% difference in the ionic radii of La to Ba but nearly a 28% difference for Sm to Ba. However, the solubility limit in the Sm123ss samples annealed in 0.01 bar PO_2 is only ≈ 0.15 (versus 0.7 for La123ss and 0.6 for Nd123ss in 0.01 bar PO_2) as determined by DTA performed under 1% O_2 (with N2 balance) flowing gas (Fig. 1). The solubility limit was determined by the presence of endothermic events prior to the peritectic decomposition of the single phase Sm123ss which occurs above 1001°C. The peritectic temperature decreases with increasing x. XRD was used to determine the second phases, which were Sm_2BaCuO_5 (Sm211) and CuO in addition to Sm123ss. The small endotherms occurring at about 885°C for $x \geq 0.2$ are peritectic reactions (p1 and p2) of Sm123 and Sm211 with CuO. As expected, the size of p1 and p2 increases with increasing $x > 0.2$. No other decomposition events were

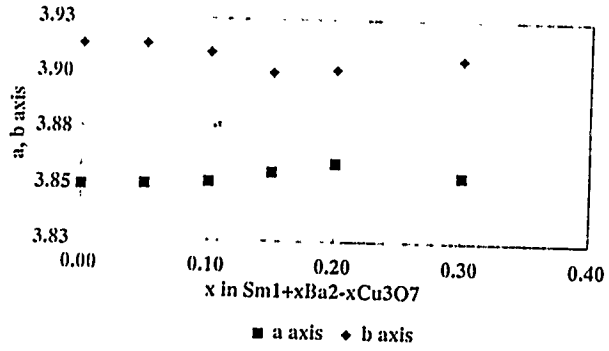

Fig. 2 XRD of Sm123ss processed in 0.01 bar PO_2.

observed by DTA for x up to 0.3. XRD showed that the amounts of Sm211 and CuO increased relative to Sm123ss with increasing x for x > 0.2. The occurrence of the Sm211 in the XRD coincided closely with the first observation of p1 by DTA. The onset for the peritectic decomposition (m1) in 0.01 bar PO_2 was 1001-1031°C versus 1050-1090°C for 1.0 bar PO_2. The presence of Sm211 and CuO in equilibrium with Sm123ss for 0.01 bar PO_2 is at odds with earlier work done at 1.0 bar PO_2 where Sm_2CuO_3 (Sm201) was observed in equilibrium with Sm123ss [5].

Lattice parameters (a and b axis) for fully oxygenated samples after the 950°C anneal in 0.01 bar PO_2 show a smooth decrease in orthorhombicity up to the solubility limit (x = 0.2) as determined by DTA (Fig. 2). Beyond this value, there is some divergence in a and b axis. In addition, there are non-systematic changes in the lattice parameters and peak intensities with increasing x. Magnetization measurements indicate a different superconducting phase occurring in these samples with x > 0.3. It is postulated that this may be Sm124. Details of this transformation will be dealt with in a latter paper.

Gd123ss

The solubility limit in the Gd123ss system in 1.0 bar PO_2 is x ≈ 0.2, a considerable decrease from the solubility limit of Sm123ss. To determine the limit of solubility in 0.01 bar PO2, DTA for the Gd123ss samples were performed in 1% O_2-balance N_2 (Fig. 3). XRD was also performed on samples annealed in 0.01 bar. The first occurrence of p1 in the DTA's occurs at x = 0.06. By extracting the area of p1 for values of x up to 0.1 and plotting that value versus x, a better determination of the solubility limit can be made. This method put the limit at 0.04 which was qualitatively confirmed by XRD. In addition to Gd211, CuO was also present in equilibrium with Gd123ss as in the Sm system.

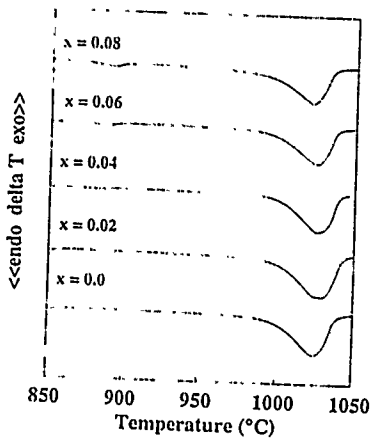

Fig. 3 DTA of Gd123ss performed in 1% O_2 balance N_2 showing the presence of a second phase occurring at x > 0.04.

Figure 4 shows the change in the a and b axis lattice parameters for x = 0.0 to 0.2 for samples processed in 1.0 and 0.01 bar PO_2. In the case of samples processed in 1 bar oxygen, there is a smooth contraction in the orthorhombicity with the sample becoming tetragonal at x = 0.20. The loss of orthorhombicity occurs at a smaller value of x for Gd123ss than for Nd123ss (x = 0.25) but similar to La123ss (x = 0.20). However, obtaining homogeneous and fully oxygenated samples in the LRE123 system has proven difficult, so

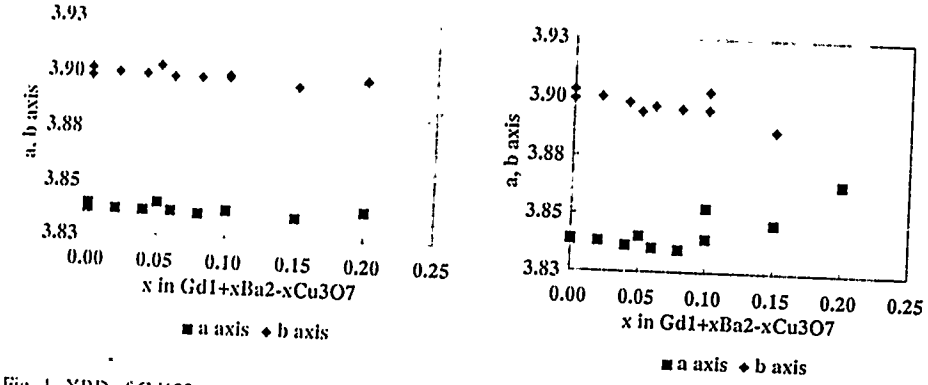

Fig. 4 XRD of Gd123ss a) processed in 1.0 bar PO_2 and b) processed in 0.01 bar PO_2.

comparisons of structural parameters from various sources is suspect. However, these data indicate that lattice parameters, hence superconductivity, can be tailored by altering LRE composition and PO_2.

DISCUSSION

Earlier work showed that the phase relationships in the La, Pr and Nd-Ba-Cu-O systems are not identical, even for those sub-solidus compositions around the LRE123ss [1-7]. Figure 5 shows the sub-solidus phase relationships for Pr-Ba-Cu-O and Nd-Ba-Cu-O systems in air at 950°C. While both systems show considerable solubility for the LRE on the Ba site in the LRE123ss, the equilibrium phase assemblages are very different. In particular, note that the LRE211 structure does not exist in either of these two systems. Since Pr123 is not superconducting, various studies have used Pr doped RE123 to probe the nature of the charge transfer in these ceramics. Although Pr readily substitutes for the other RE's, high doping levels of Pr could result in subtle, complex microstructures. For instance, a nominal substitution of Pr for Ba in Nd123ss results in a very different structure than nominal substitution of Pr for Nd in Nd123ss [13]. Thus, an understanding of these variations in the phase relationships must be taken when doing experiments in the Pr doped LRE123 systems.

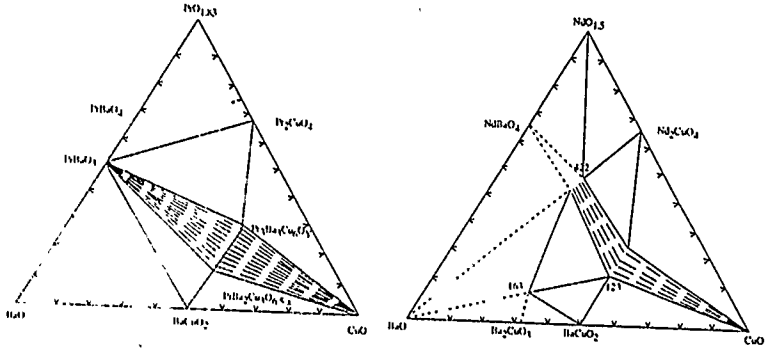

Fig. 5 Sub-solidus phase realtionships in the Pr-Ba-Cu-O [7] and Nd-Ba-Cu-O [8] systems.

Table 1. Solid solubility limits for LRE in the Ba sites in $LRE_{1+x}Ba_{2-x}Cu_3O_{7+\delta}$

LRE	Ionic Radii	Lower Limit	Upper Limit	Temperature (°C)	PO_2 (bar)
La[3]	1.061	0.02	0.70	977	1.0
Pr[7]	1.013	0.02	0.70	880	0.01
		0.01	na		0.2
		0.03	0.7		1.0
Nd[5,8]	0.995	0.01	0.7	890	0.01
		0.04	0.60		0.2
		0.03	0.38	950	1.0
Sm[12]	0.964	0.00	0.60	940	.001
		0.00	0.70	1025	1.0
Eu[3]	0.950	0.00	0.15	950	0.01
		0.0	0.25	950	1.0
Gd[6]	0.938	0.0	0.1	940	0.01
		0.0	0.20	950	1.0
		0.0	0.04	950	0.01

The sub-solidus equilibrium phases in the Sm and Gd-Ba-Cu-O also differ from the La, Pr and Nd-Ba-Cu-O systems. One of the biggest changes going from Nd to Sm-Ba-Cu-O is the formation of the line compound Sm211 which is now in equilibrium with $BaCuO_2$ (011) and Sm123. In the Sm and Gd-Ba-Cu-O system, the phase relationships around the LRE123ss structure are similar in 0.01 bar PO_2 but, as noted above, the equilibrium phases around Sm123ss changes with PO_2 (Fig. 6). The solubility limit drastically decreases with the lower PO_2 . The experimentally determined values for x are given in Table 1. Of particular interest is the three phase region beyond the upper solubility limit. While the upper limit to the solubility varies from LRE to LRE, the same two phases are in equilibrium with LRE123ss, LRE211 and CuO. The peritectic decomposition of LRE123ss $\Leftrightarrow$ LRE211 + CuO + ℓ where the amount of solubility can be controlled by PO_2, mixtures of LRE or both. The dependence of the solubility on PO_2 and LRE will be discussed below.

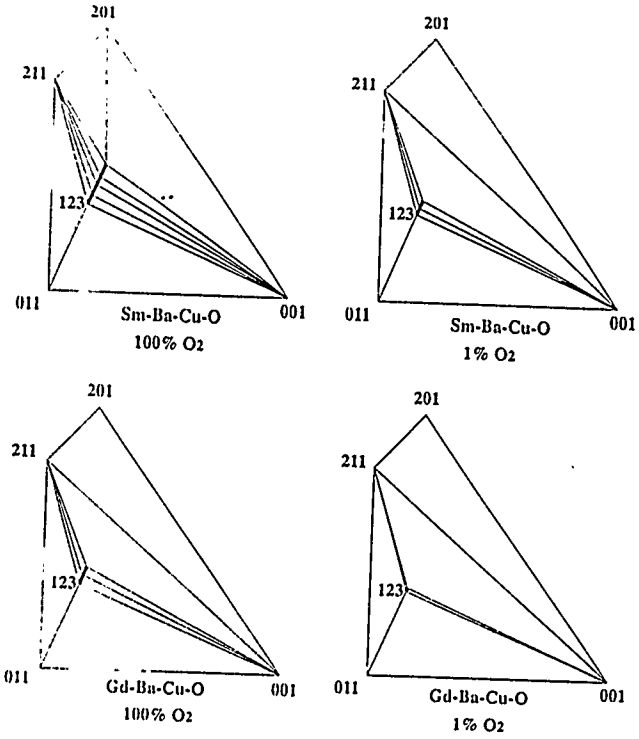

Fig. 6 Partial ternary diagrams for the Sm and Gd systems showing the sub-solidus phase relationships around the LRE123ss. The heavy line indicates the limit of the solubility.

The fact that at PO_2 = 1 bar stoichiometric LRE123 (x = 0) for LRE = La, Pr, Nd is not stable indicates a strong affinity of the LRE for the Ba site, regardless of the higher valence state. This affinity is stronger for the larger ions as indicated by their larger solubility limits. The ability of the LRE to substitute for the Ba appears to be based solely on ionic radii size since electronegativity and valence (in most cases) does not change for the lanthanides. For those ions where the valence can change (i.e., Pr and Eu) there is no clear evidence that these ions are other than in the 3+ state. As the ionic radii decreases, the RE-O bonds are strained. For the larger LRE, this strain is smaller, allowing for a higher solubility. At some point the lattice strain exceeds the entropy saved by forming a solid-solution and the LRE123ss collapses down to a line compound.

In addition to the size effect, the 3+ charge of the RE requires extra oxygen be incorporated into the structure to compensate the charge. In the defected triple Pervoskite structure, this is not a problem due to the mobility of the

oxygen in the chain and anti-chain sites. For x = 0, it is known that increasing temperature or decreasing PO_2 reduces the chain-site (O_1) occupancy resulting in a tetragonal symmetry. Incorporating excess RE into the 123 structure should counteract the loss of the O_1 oxygen. This effect has been investigated in the La123ss over a range of PO_2's and T's [3]. It has been well established that in oxygenated LREss δ is ~ 0.5x [3,9]. At high temperatures, there are competing effects. Thus it is expected that the isopleths for δ would shift downward on the PO_2 vs 1/T phase diagram while at the same time the peritectic decomposition temperature decreases. This would imply that the more heavily substituted structures become unstable when there is insufficient oxygen to stabilize the RE on the Ba site. Since each RE on a Ba site produces only one extra electron, one O atom is added to the structure for every two RE. If the two RE's are on adjacent Ba sites, local charge balance is maintained. However if the Ba sites are randomly populated by RE ions, the situation is more complex. If an O atom is added to the unit cell, it can expect one electron from the RE. The other electron must come from increasing the valence of the Cu ions. If on the other hand, no O is added to the unit cell, the RE electron decreases the valence of the Cu. Since reducing Cu in an oxidizing atmosphere seems unlikely, it is reasonable to assume that an O is always added to the unit cell containing the excess RE. In lower PO_2, there is simply not enough oxygen activity to maintain the proper Cu valence state and the structure breaks down. The ability of the LRE's to pair or populate the Ba sites randomly would be dependent on both temperature and PO_2. This is a reasonable explanation for sample variability noted in the literature. In addition, how the LRE occupy the Ba sites also has been implicated in the variability in the superconducting transition temperature for the same material processed at different temperatures and oxygen partial pressures [9,10].

CONCLUSIONS

For the light rare earth elements (LRE), there is a varying degree of solubility of the LRE^{3+} ions for Ba^{2+} ions in the $LREBa_2Cu_3O_7$ structure forming a solid solution $LRE_{1+x}Ba_{2-x}Cu_3O_{7+\delta}$ (LRE123ss), with increasing substitution of the LRE^{3+} for the Ba^{2+} with increasing ionic radii of the LRE. The sub-solidus phase relationships around the LRE123ss change for La, Pr and Nd, but are similar for Sm, Eu and Gd. However, the solubility limit decreases with decreasing ionic radii. In addition, the solubility limits for Sm, Eu and Gd are strongly influenced by PO_2 during high temperature annealing. Understanding the subtle phase relationships provides a new means by which to control the microstructure in the RE123 system.

ACKNOWLEDGMENTS

The work was performed at Ames Laboratory, Iowa State University was supported by the Director of Energy Research, Office of Basic Sciences, U.S. Department of Energy under Contract No. W-7405-ENG-82.

REFERENCES

1 R.D. Shannon and C.T. Prewitt, Acta. Cryt., B25, 925 (1969).
2 K. Takita, H. Akinaga, H. Katoh and K. Masuda, Jpn. J. Appl. Phy., 27, L1676 (1988).
3 T.B. Lindemer, E.D. Specht, C.S. MacDougall, G.M. Taylor and S.L. Pye, Physica C, 216, 99 (1993).
4 W. Wong-Ng, B. Paretzkin and E. R. Fuller, Jr, J. Sol. Sta. Chem. 85 ,117 (1990).
5 P. Karen, O. Braaten and A. Kjekshus, Acta Chem. Scand., 46, 805 (1992).
6 M. D. Hill, W. K. Wong-Ng, C.K. Chiang, E.R. Fuller, B. Paretzkin, J. E. Blendell, E. Lagergren and R. Kacker, J. Am. Ceram. Soc., 75, 2390 (1992).
7 M. Park, M.J. Kramer, K.W. Dennis and R.W. McCallum, submitted to Physica C
8 S. I. Yoo amd R.W. McCallum, Physica C, 210, 147 (1993).
9 M.J. Kramer, S.I. Yoo, R.W. McCallum, W.B. Yelon, H. Xie, and P. Allenspach, Physcia C, 219, 145 (1994).
10 R.W. McCallum, M.J. Kramer, K.W. Dennis, M. Park, H. Wu and R. Hofer, J. Elec. Mat (in press)
11. K. Zhang, B. Dabrowski, C. U. Segre, D.G. hinks, I.K. Schuller, J.D. Jorgensen and M. Slaski, J. Phys. C20, L935 (1987).
12 W. Wong-Ng, B. Paretzkin and R. Fuller, Advances in X-ray Analysis, 33, 453 (1990).
13 M.J. Kramer (unpublished work).